http://dx.doi.org/10.11142/jicems.2013.2.2.127
*Journal of International Conference on Electrical Machines and Systems Vol. 2, No. 2, pp. 127~133 , 2013* **127**

# Design of Surface Permanent Magnet-type Vernier Motor

**Hironori Kakihata *, Yasuhiro Kataoka *, Masakazu Takayama *, Yoshitarou Matsushima ** and Yoshihisa Anazawa ***

**Abstract – In this paper, the authors designed a surface permanent magnet (SPM)-type vernier motor whose maximum output is more than 5.2 kW, whose power factor at 4 kW is more than 90%, and whose efficiency at 4 kW is 85% under the conditions that the operating voltage, frequency, and synchronous speed are 400 V, 50 Hz, and 100 min-1, respectively.**

**Keywords: Surface permanent magnet type, Vernier motor, Design, Output characteristics**

## 1. Introduction

In drive systems such as a traction machine for elevators, in which a high torque must be generated at low speeds, a reduction gear is generally used. However, a reduction gear has problems such as backlash, friction loss, and maintenance. To solve these problems, research on direct-drive systems has been conducted. To connect a motor directly with a load without using a reduction gear, a motor should generate high torque at a low speed. Although the stepping motor and the brushless DC motor are used for direct drive systems, these motors have a pulsating torque. So, various vernier motors, which theoretically have no pulsating torque, have been developed [1]-[4].

In recent years, the performance of a motor using a permanent magnet has been improved by increasing the energy product of the permanent magnet. In the vernier motor, a surface permanent magnet (SPM) type has been developed. But as Toba et al. [3] reported, a low power factor of 56% remains problematic.

In our laboratory, the output characteristics calculation method, which use a voltage equation on the γ-δ axis and a torque equation, has been proposed [5], [6]. In this study, the induced electromotive force and the synchronous reactance, which are used on a voltage equation and a torque equation, are calculated by the finite element method (FEM) analysis. The advantages of using the voltage equation and the torque equation are the small calculation scale and the intuitive understanding of the result. However, the influence of magnetic saturation and iron loss cannot be considered in this method. Therefore, it is necessary to calculate the output characteristics by FEM analysis directly [7].

* Dept. of Electronics and Information Systems, Akita Prefectural University, Japan. (yasuhiro_kataoka@akita-pu.ac.jp, masat@akita-pu.ac.jp, anazawa@akita-pu.ac.jp)

** Dept. of Electrical and Electronic Engineering, Shizuoka University, Japan. (teymats@ipc.shizuoka.ac.jp)

Received 12 November 2012 ; Accepted 25 January 2013

## 2. Principle and torque equation

### 2.1 Operating Principles of an SPM-type Vernier Motor

The basic composition of an SPM-type vernier motor is shown in Fig. 1. The number of slots is 6, and the number of rotor poles is 10. A three-phase armature coil of the full pitch winding is specified for the stator slot. The permanent magnets are set on the surface of the rotor core so that the North pole and the South pole appear alternately. The relation of *S*, *R*, and P is denoted in (1), where *S* is the number of slots of the stator, *R* is the number of poles of the rotor, and *P* is the number of poles of the rotating magnetic field.

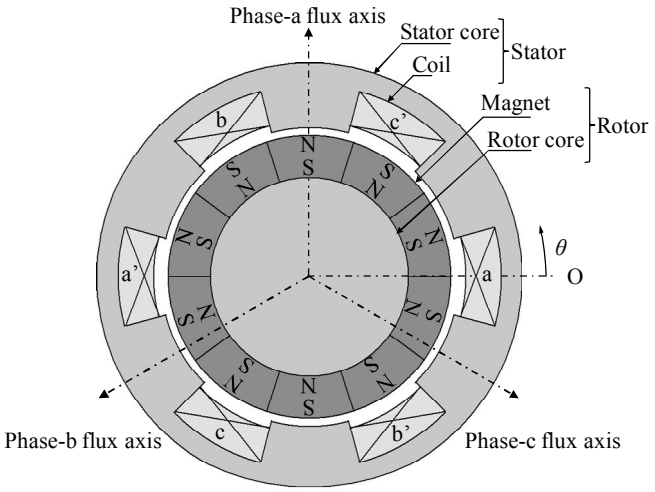


**Fig. 1.** Structure of an SPM-type vernier motor

$$S = \frac{R}{2} \pm \frac{P}{2} \tag{1}$$

Fig. 2, which shows the linear operation of Fig. 1, is the principle of operation of an SPM-type vernier motor. In this figure, the magnetomotive force and the magnetic flux density distribution for $i_a = -2i_b = -2i_c$ were shown. Additionally, the currents of the a phase, the b phase, and the c phase, denoted by $i_a$, $i_b$, and $i_c$, respectively.

Because there are slots and teeth in the stator, gap permeance pulsates periodically. Therefore, the magnetomotive force is modulated by gap permeance, and the magnetic flux density of the gap contains the fundamental wave, the 5th wave, and the 7th wave. Then, the rotor synchronizes with the 5th wave, because rotor has 10 poles. The synchronous speed $N$ is denoted by (2), where $f$ is the frequency, because the rotor rotates at $P/R$ times the speed of the rotating magnetic field generated by the armature coil. So, the SPM-type vernier motor can realize super slow speed rotation easily by increasing the number of poles of the rotor:

$$N = \frac{120f}{P}\frac{P}{R} = \frac{120f}{R} \tag{2}$$

### 2.2 Derivation of the Torque Equation

The voltage equation on the γ-δ axis and the torque equation in an SPM-type vernier motor have been explained more fully in past papers [5], [6].

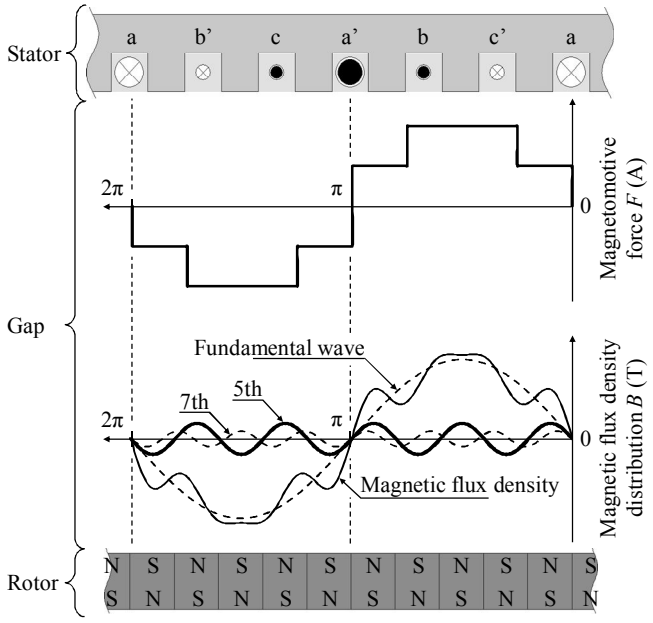


**Fig. 2.** Principle of an SPM-type vernier motor

The voltage equation of an SPM-type vernier motor in the steady state on the γ-δ axis is denoted by (3) and (4).

$$V\sin\left(\frac{R}{2}\delta_L\right) = -r_a I\sin\left(\varphi - \frac{R}{2}\delta_L\right) + X_S I\cos\left(\varphi - \frac{R}{2}\delta_L\right) \tag{3}$$

$$V\cos\left(\frac{R}{2}\delta_L\right) = X_S I\sin\left(\varphi - \frac{R}{2}\delta_L\right) + r_a I\cos\left(\varphi - \frac{R}{2}\delta_L\right) + E_0 \tag{4}$$

(5) and (6) are obtained if (3) and (4), respectively, are solved for the current:

$$I\sin\left(\varphi - \frac{R}{2}\delta_L\right) = \frac{V}{Z}\sin\left(\varphi_S - \frac{R}{2}\delta_L\right) - \frac{E_0}{Z}\sin\varphi_S = -\frac{I_\gamma}{\sqrt{3}} \tag{5}$$

$$I\cos\left(\varphi - \frac{R}{2}\delta_L\right) = \frac{V}{Z}\cos\left(\varphi_S - \frac{R}{2}\delta_L\right) - \frac{E_0}{Z}\cos\varphi_S = -\frac{I_\delta}{\sqrt{3}} \tag{6}$$

where $V$ is the operating voltage (V), $r_a$ is the resistance of the armature coil (Ω), $X_S$ is the synchronous reactance (Ω), $Z = \sqrt{r_a^2 + X_S^2}$, $\varphi_S = \tan^{-1}(X_S / r_a)$, $E_0$ is the induced electromotive force (V), $\varphi$ is the power factor angle (rad), $R\delta_L/2$ is the power angle (rad), $I_\gamma$ is the current of the γ axis (A), and $I_\delta$ is the current of the δ axis (A).

The torque equation and the induced electromotive force equation are shown in (7) and (8), respectively:

$$T = -\left(\frac{R}{2}\right)M_F I_F I_\delta \tag{7}$$

$$E_0 = \frac{\omega}{\sqrt{3}}M_F I_F \tag{8}$$

where $\omega$ is the angular frequency (rad/s), and $M_F I_F$ is the flux linkage (Wb).

The equations of the torque and the output are shown by (9) and (10) from (6), (7), and (8).

$$T = \frac{3}{\omega}\frac{R}{2}\left\{\frac{VE_0}{Z}\cos\left(\varphi_S - \frac{R}{2}\delta_L\right) - \frac{E_0^2}{Z}\cos\varphi_S\right\} \tag{9}$$

$$P_O = 3\left\{\frac{VE_0}{Z}\cos\left(\varphi_S - \frac{R}{2}\delta_L\right) - \frac{E_0^2}{Z}\cos\varphi_S\right\} \tag{10}$$

Moreover, the output $P_O$ is denoted in equation (11) if the resistance of the armature coil $r_a$ is ignored.

$$P_O = 3\left(\frac{VE_0}{X_S}\sin\frac{R}{2}\delta_L\right) \tag{11}$$

The output of an SPM-type vernier motor has the same form as that of the common synchronous motor.

## 3. Design and Calculation Method

In this chapter, the design concept of an SPM-type vernier motor is explained. And output characteristics are calculated by FEM analysis.

### 3.1 Design Concept of the SPM-type Vernier Motor

For equation (11), the output of the motor is proportional to the induced electromotive force and inversely proportional to the synchronous reactance under a constant operating voltage $V$. For the induced electromotive force $E_0$ and the synchronous reactance $X_S$, (12) to (15) are known:

$$E_0 \propto n \tag{12}$$

$$E_0 \propto l \tag{13}$$

$$X_S \propto n^2 \tag{14}$$

$$X_S \propto l \tag{15}$$

where $n$ is the number of armature coil turns (turn), and $l$ is the core length (m).

Therefore, the output does not change with the core length and the output is inversely proportional to the number of armature coil turns.

Additionally, the power factor is maximized and the current is minimized when the induced electromotive force $E_0$ is the same as the operating voltage $V$.

In this study, first of all, the number of turns is decided by maximum output, and secondly, the power factor is improved by adjusting the core length.

### 3.2 The Procedure of Calculation using FEM Analysis

Fig. 3 shows the calculation procedure for calculating the output characteristics directly by 2D FEM analysis [7]. In this method, torque and current are calculated directly by accounting for the external voltage source. This causes a lengthy calculation time. Additionally, to determine the optimum design parameters, numerous calculations are needed. However, this method can calculate iron loss and considers the influence of magnetic saturation.

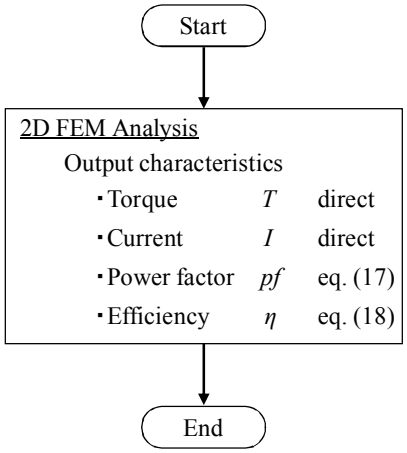


**Fig. 3.** Procedure of FEM analysis

Fig. 4 shows the phasor diagram of an SPM-type vernier motor. Power angle $R\delta_L/2$ is the phase difference of the voltage and the induced electromotive force. The torque is calculated by changing the power angle, which changes with the transition of the phase of the voltage on the basis of the induced electromotive force. In addition, in the analysis, the torque and the current were calculated at a point considered to have fully converged.

In this method, the output $P_O$, the power factor $pf$, and efficiency $\eta$ are calculated by (16), (17), and (18), respectively:

$$P_O = T\frac{2\pi N}{60} = T\frac{2\pi}{60}\frac{120f}{R} = T\frac{2\omega}{R} \tag{16}$$

$$pf = \cos\varphi = \frac{1}{VI}\left(\frac{P_O}{3} + r_a I^2\right) \tag{17}$$

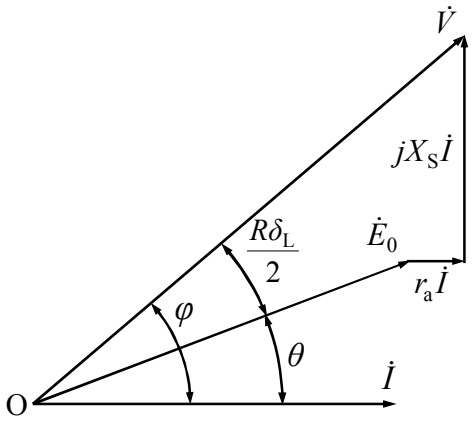


**Fig. 4.** Phasor diagram of SPM-type vernier motor

$$\eta = \frac{P_O - P_i}{P_O + 3r_a I^2} \tag{18}$$

where $T$ is the torque (N·m), $\omega$ is the angular velocity (rad/s), $r_a$ is the resistance of the armature coil at 75˚C (Ω), $I$ is the current (A), $\eta$ is the efficiency (%), and $P_i$ is the iron loss (W).

This method has the following advantages: the influence of magnetic saturation and the iron loss can be considered. However, the disadvantages are that the FEM analysis scale becomes large, and the relation between the output results of FEM analysis and the design parameter is unclear.

### 3.3 Consideration of the Coil-end Leakage Reactance

In this calculation method, a coil-end leakage reactance is considered in the 2D FEM analysis. The coil-end leakage reactance coil is connected in series to "FEM coil" in the analysis (JMAG studio Ver. 10.0). The inductance of the coil-end leakage reactance is calculated by Kilgore's (19) and (20) [8]:

$$x_l = X\lambda_e = X\frac{4}{l}(2l_{e2} + l_{e1}) \tag{19}$$

$$X = 40flm(2p)\left(q\frac{n_s}{c}k_p k_d\right)^2 \times 10^{-8} \tag{20}$$

where λe is the permeance of the coil-end leakage, (2le2+le1) is the measurement of the coil end, X is the leakage coefficient, q is the number of slots per pole per phase (=1), m is the number of phases (=3), c is the number of parallel circuits per phase (=1), ns is the number of conductors in each slot (Type I : 56, Type II : 76), p is the number of pole pairs (=6), kp is the short pitch factor (=1), and kd is the distribution factor (=1).

### 3.4 Specifications of the Designed Model

Table 1 shows the specifications of an SPM-type vernier motor for the Type I and Type II models. Type I is the old model that designed to generate a high torque, and Type II is the new model that designed to improve the output characteristics. The number of armature coil turns of Type II is set to be 1.3 times that of Type I, because the operating voltage is increased from 300 to 400 V (1.3 times). The core length of Type II is set to be 2.0 times that of Type I to improve the power factor. By increasing the core length, the induced electromotive force increases (denoted in (13)), so that it becomes approximately equal to the operating voltage.

**Table 1** Specifications of the type I and II models

| Type | | I | II |
|---|---|---|---|
| Operating voltage | (V) | 300 | 400 |
| Number of armature coil turns | (turn) | 336 | 456 |
| Core length | (mm) | 60 | 120 |
| Induced electromotive force | (V) | 142 | 385 |
| Resistance of armature coil (75˚C) | (Ω) | 0.98 | 1.78 |
| Frequency | (Hz) | 50 | |
| Synchronous speed | ($min^{-1}$) | 100 | |
| Residual induction of magnet | (T) | 1.45 | |
| Coercive force of magnet | (kA/m) | 1074 | |
| Material of core | — | 50A290 | |
| Number of slots | — | 36 | |
| Number of rotor poles | — | 60 | |
| Number of poles | — | 12 | |

Fig. 5 shows the 1-pole section of the motor component. Type I and Type II have the same cross section. The radius of stator is 200 mm, the number of slots is 36, the number of rotor poles is 60, and the number of poles is 12. The stator has the three phase armature windings. The demagnetization areas of the permanent magnet and the glue layer are also considered. Fig. 6 shows the magnetization model of the permanent magnet. The arrows show the magnetomotive force by the permanent magnet. The demagnetization areas are set at a width of 1/4 pole pitches from both sides of the magnets, and the magnetomotive force decreases linearly.

### 3.5 Consideration of the Coil-end Leakage Reactance

Fig. 7 shows the comparison of output characteristics calculated by FEM analysis. The output characteristics of Type II are improved from those of Type I. The maximum

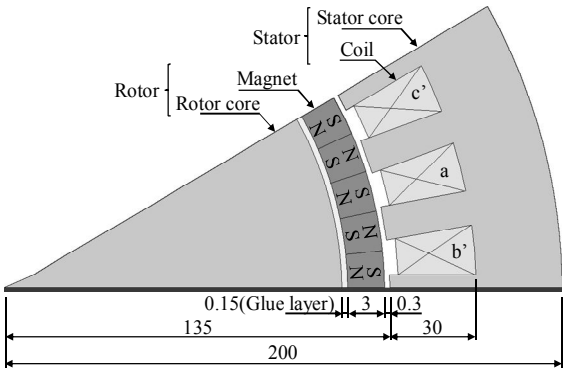


**Fig. 5.** 1-pole section of the motor component (Units: mm)

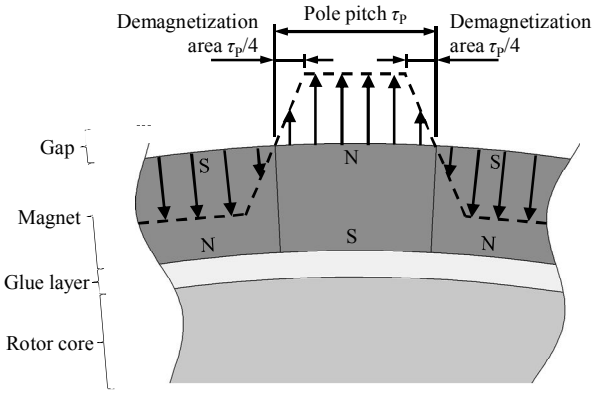


**Fig. 6.** Magnetization model of the permanent magnet

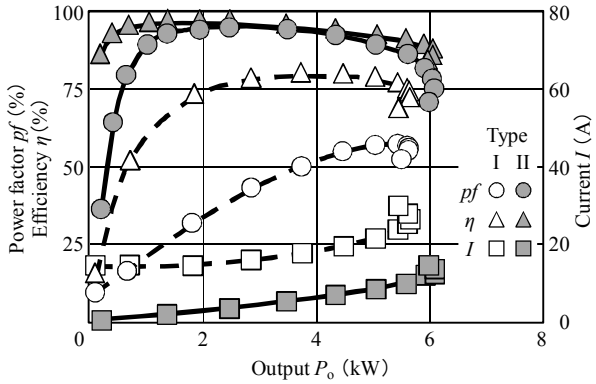


**Fig. 7.** Comparison of output characteristics calculated by FEM analysis

output of 6.1 kW is obtained in Type II. Table 2 shows the output characteristics at 4 kW. The power factor is 93.0% and the efficiency is 93.6% in Type II. So, the design objective is attained in Type II.

### 3.6 Investigation of the Magnetic Flux Density

Fig. 8 and Fig. 9 show the magnetic flux lines of the Type I and Type II, respectively. The magnetic flux density of the tooth is 1.25 T in Type I and 0.65 T in Type II. Moreover, in the backyork, the magnetic flux density is 0.29 T in Type I and 0.15 T in Type II. Accordingly, the Type II has low magnetic flux density compared with Type I.

**Table 2** Characteristics at 4 kW by FEM analysis.

| Type | | I | II |
|---|---|---|---|
| Current | (A) | 18.5 | 6.6 |
| Power factor | (%) | 52.1 | 93.0 |
| Iron loss | (W) | 40.4 | 29.1 |
| Copper loss | (W) | 1006 | 233 |
| Efficiency | (%) | 79.3 | 93.9 |

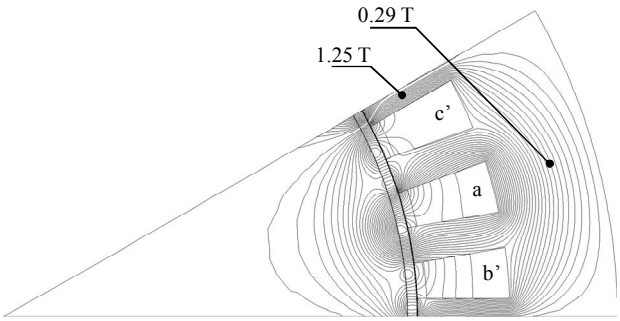


**Fig. 8.** Magnetic flux lines of Type I.
(Interval of magnetic flux lines is 0.5 mWb/line)

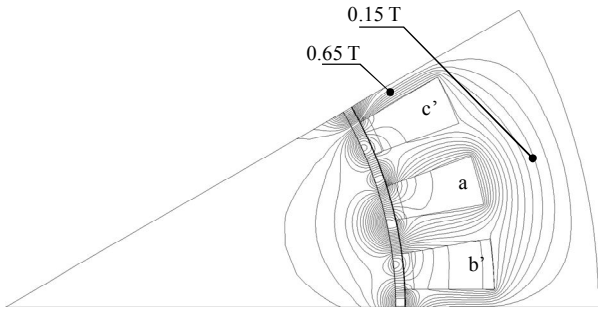


**Fig. 9.** Magnetic flux lines of Type II
(Interval of magnetic flux lines is 0.5 mWb/line)

## 4. Characteristics Calculation by the Torque Equation

In this chapter, the output characteristics of Type I and Type II are calculated by proposed method using the torque equation. Then, the accuracy of the proposed method is checked by comparing it with FEM analysis of chapter III.

### 4.1 The Procedure of Calculation using the Torque Equation

Fig. 10 shows the procedure of the proposed method. In this method, induced electromotive force and synchronous reactance are calculated by the FEM. Therefore, the calculation time is short. And the output is obtained by substituting the induced electromotive force and the synchronous reactance into equation (10). The output characteristics (power factor, efficiency, and current) are calculated by equations (5), (6), and (18). The proposed method has the advantage that the influence of design parameters, which affect the output, can be easily estimated from equation (11). Accordingly, the proposed method is useful in the design of SPM-type vernier motors. However, accurate calculations that consider magnetic saturation are

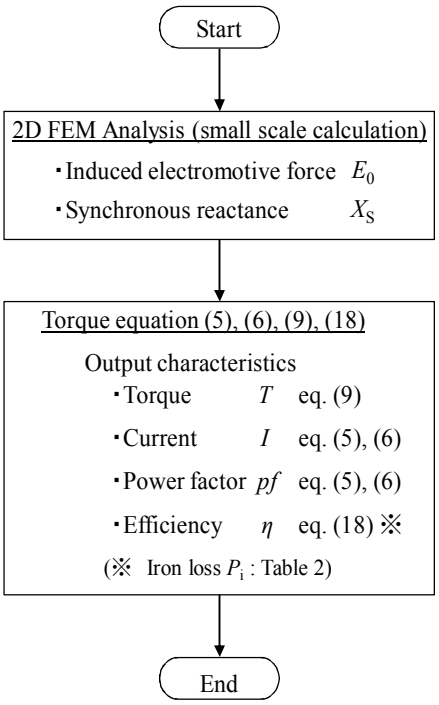


**Fig. 10.** The procedure of the proposed method

difficult, and iron loss can be calculated using other methods. Therefore, efficiency is calculated using the iron loss obtained by FEM analysis (Table 2).

### 4.2 Calculation Results of the Proposed Method

Fig. 11 shows the comparison of output characteristics calculated by the proposed method. The maximum output is 6.4 kW in Type II. Table 3 shows the output characteristics at 4 kW, including the iron loss and the copper loss. The power factor at 4 kW is 95.6% and the efficiency at 4 kW is 94.2% in Type II.

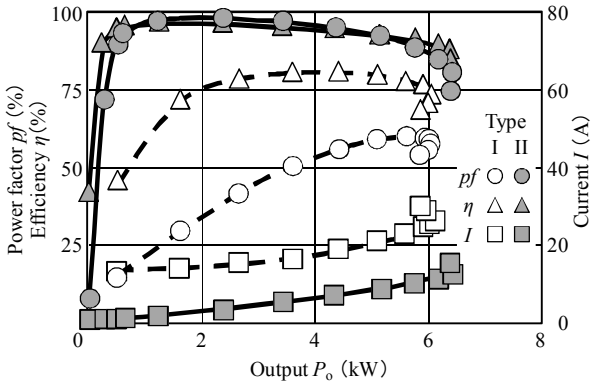


**Fig. 11.** Comparison of output characteristics calculated by the proposed method

**Table 3** Characteristics at 4 kW by proposed method

| Type | | I | II |
|---|---|---|---|
| Current | (A) | 17.8 | 6.4 |
| Power factor | (%) | 53.2 | 95.6 |
| Iron loss | (W) | 40.4 | 29.1 |
| Copper loss | (W) | 1006 | 233 |
| Efficiency | (%) | 80.4 | 94.2 |

### 4.3 Precision of the Proposed Method

The accuracy of proposed method is compared with FEM analysis using the Type II in Fig. 12. The lines show the output characteristics calculated by the proposed method, and the plotted points show the results calculated by FEM analysis directly. The output characteristics agree well, although the difference becomes large near the maximum output. Therefore, the calculation method by the proposed method has sufficient accuracy.

## 5. Conclusions

In this study, the authors designed an SPM-type vernier motor and confirmed that the design objective was attained. Also, the results of FEM analysis and those of the proposed method were compared. The results are as follows.

The output did not change with the core length and the output was inversely proportional to the number of armature coil turns. Because induced electromotive force was proportional to the core length and the number of armature coil turns, and synchronous reactance was proportional to core length and the square of the number of armature coil turns. Therefore, output characteristics of designed motor were improved by adjusting the core length and the number of turns. As a results, the design objective was attained.

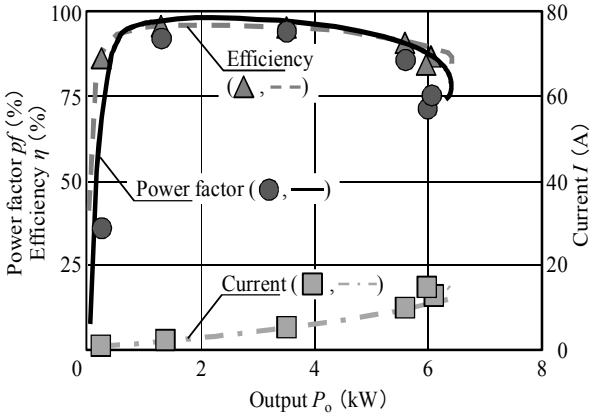


**Fig. 12.** The precision of proposed method (Type II)

Comparing proposed method with FEM analysis, accuracy of the proposed method is excellent, therefore, the proposed method is applicable to the design of the SPM-type vernier motor.

The design process using FEM analysis is large scale simulation with long-run calculation, therefore, the proposed method can permit greatly accelerating the design process, because this method has the advantage of the small scale calculation.

In the future, authors will consider an optimum design for achieving high torque.

## References

[1] A. Ishizaki, Y. Shibata, K. Watanabe, and K. Saitoh, "Low-speed High-torque Drive System Applying Vernier Motor Torque," T. IEE Japan, Vol. 111-D, No. 9, pp. 785-793, September, 1991.

[2] A. Ishizaki, T. Tanaka, K. Takasaki, S. Nishikata, and A. Katagiri, "Theory and Torque Characteristics of PM Vernier Motor," T. IEE Japan, Vol. 113-D, No. 10, pp. 1192-1199, October, 1993.

[3] A. Toba, T. Watanabe, Y. Koganei, and H. Ohsawa, "Design and Experimental Evaluation of 5 kW-Surface Permanent Magnet Vernier Machines," T. IEE Japan, Vol. 122-D, No. 2, pp. 162-168, February, 2002.

[4] Y. Anazawa, K. Tajima, A. Kaga, Y. Ito, and H. Isozaki, "Analysis of Vernier Motors Based on the Unified Theory," T. IEE Japan, Vol. 113-D, No. 11, pp. 1317-1323, November, 1993.

[5] H. Suda, Y. Matsushima, and Y. Anazawa, "A Study of Analysis and Characteristic of Surface Permanent Magnet Vernier Motor," Papers of the Technical Meeting on Rotating Machinery, IEE Japan RM-07-33, May, 2007.

[6] S. Takita, Y. Kataoka, M. Takayama, Y. Matsushima, and Y.Anazawa, "Design of High Torque Surface Permanent Magnet Type Vernier Motor - Effects of Inside Radius on Pull-out Torque in Outer Rotor Type," The Papers of the Technical Meeting on Rotating Machinery, IEE Japan RM-11-97, October, 2011.

[7] H. Kakihata, Y. Kataoka, M. Takayama, Y. Matsushima, and Y. Anazawa, "Calculation of Pull-out Torque and Output Characteristics Using Finite Element Method in Surface Permanent Magnet Type Vernier Motor," The Papers of the Technical Meeting on Rotating Machinery, IEE Japan RM-11-96, October, 2011.

[8] IEE Japan, "Design of electrical machinery and apparatus," 1982.

**Hironori Kakihata** He received MA degree in electrical engineering from Akita prefectural University. His research interests are design of surface permane nt magnet-type vernier motor.

**Yasuhiro Kataoka** received Dr. Eng. degree from Shinshu University, Nagano, Japan, in 2003. He joined Tamagawa seiki Co. Ltd. from 2003 to 2010. Since 2010, he has been an Assistant Professor at the Akita Prefectural University. His research interests include analysis and design of electric machines.

**Masakazu Takayama** received Dr. Eng. degree from Tohoku University in 1991. Since 2000, he has been an Associate Professor at Akita Prefectural University. His research interests are applications of electromagnetic engineering.

**Yoshitarou Matsushima** received B.S degree in electrical engineering from Muroran Institude of Technology in 1975 and M.E degree from Hokkaido University in 1977. He is now an associate professor at Shizuoka University. His research interests are analysis and design of electric machines.

**Yoshihisa Anazawa** received Dr. Eng. degree from Hokkaido University in 1987. He became a lecturer in 1980, an Associate Professor in 1989 at the Akita University. Since 1999, he has been a Professor in Akita Prefectural University. His research interests include analysis and design of electric machines.